APRIL 1967
REPORT SM-49105-Q3

STRESS CORROSION CRACKING OF TITANIUM ALLOYS AT AMBIENT TEMPERATURE IN AQUEOUS SOLUTIONS

PROGRESS REPORT FOR PERIOD
JANUARY, FEBRUARY AND MARCH 1967
UNDER CONTRACT NAS 7-488

ASTROPOWER LABORATORY
2121 CAMPUS DRIVE • NEWPORT BEACH, CALIFORNIA

MISSILE & SPACE SYSTEMS DIVISION
DOUGLAS AIRCRAFT COMPANY, INC.
SANTA MONICA/CALIFORNIA

DOUGLAS

Report SM-49105-Q3

STRESS CORROSION CRACKING OF TITANIUM ALLOYS AT AMBIENT TEMPERATURE IN AQUEOUS SOLUTIONS

1 JAN 31 MAR

Quarterly Progress Report
For January, February, March 1967

Contract NAS 7-488

Administered by
Chief, Research SRT NASA Headquarters
Code RRM

Prepared by:

T. L. Mackay, Ph.D.
Senior Research Scientist

C. B. Gilpin, Ph.D.
Consultant

Approved by:

N. A. Tiner, Ph.D.
Head, Materials Department

MISSILE & SPACE SYSTEMS DIVISION
ASTROPOWER LABORATORY
Douglas Aircraft Company, Inc.
Newport Beach, California

FOREWORD

This report was prepared by the Astropower Laboratory, Douglas Aircraft Company, Inc., under NASA Contract NAS 7-488. It covers the period from January 1 through March 31, 1967. The work is administered by Chief, Research SRT NASA Headquarters, Code RRM, with Mr. W. Raring as Project Scientist. This report was prepared by Dr. T. L. Mackay and Dr. C. B. Gilpin under the direction of Dr. N. A. Tiner. Mr. R. G. Ingersoll, Mr. W. A. Cannon, and Mr. S. M. Toy have greatly contributed to the performance of this work.

ABSTRACT

Electron microautoradiograph studies of distribution of hydrogen by gas adsorption in titanium alloys showed: (1) a uniform distribution in Ti-13V-11Cr-3Al alloy, (2) a concentration of hydrogen in beta phase of Ti-8Al-1Mo-1V and Ti-6Al-4V alloys, and (3) a segregation of hydrogen at beta precipitates in alpha grain boundaries in Ti-5Al-2.5Sn.

Stress corrosion tests in distilled water and in 3% NaCl aqueous solution at ambient temperature were made employing single edge notch specimens of Ti-5Al-2.5Sn, Ti-6Al-4V, Ti-8Al-1Mo-1V, and Ti-13V-11Cr-3Al. The beta alloy, Ti-13V-11Cr-3Al, was the only material which showed good resistance to stress corrosion cracking in these environments. Electron microfractographs of stress corrosion fractures of alpha and alpha-beta alloys showed a mixture of cleavage and ductile dimple rupture. Cleavage areas were larger in salt solution tests. Profiles of the stress corrosion fractures of Ti-5Al-2.5Sn and Ti-6Al-4V show beta phase does not exhibit ductility, and cleavage occurs at the alpha-beta phase boundaries in the stress corrosion fracture. The preferential segregation of hydrogen in the beta phase appears to be associated with this local cleavage.

TABLE OF CONTENTS

LIST OF ILLUSTRATIONS

LIST OF TABLES

1.0 INTRODUCTION AND SUMMARY

Titanium alloys are found susceptible to stress corrosion cracking at ambient temperature in aqueous solutions. This may be a serious problem in spacecraft and proposed supersonic transport applications, and very little is known about the nature of susceptibility to stress corrosion cracking.

The objectives of this program are to conduct a detailed literature survey and to carry out an experimental program to define the microprocesses in stress corrosion failure of different titanium alloys at ambient temperature in aqueous salt solutions. The experimental methods used for these evaluations include (1) examination of stress corrosion cracked surfaces by microfractography, (2) determination of preferential attack by transmission electron microscopy, (3) determination of the role of hydrogen, if any, by electron microautoradiography, and (4) evaluation of possible electrochemical reactions by potentiostatic measurements. The techniques of using these experimental methods were developed previously in other programs conducted by Astropower Laboratory on stress corrosion cracking of high strength steels.[1]

The work reported during this quarterly period deals with the determination of K_c values for titanium alloys in air and aqueous solutions to evaluate their susceptibility to stress corrosion cracking. Electron fractographic studies were made of the stress corrosion fracture faces to determine crack propagation paths in air and aqueous environments. Microautoradiographic examination was completed of tritium, introduced into titanium alloys by gas adsorption at 725°, to determine the preferential retention of hydrogen in the various phases present in titanium alloys.

2.0 EXPERIMENTAL EVALUATIONS

2.1 Selected Alloy Sample Characteristics

The following titanium alloys were selected for detailed investigation of the mechanism of stress corrosion cracking.

1. Ti-5Al-2.5Sn, all-alpha alloy
2. Ti-6Al-4V, alpha-beta alloy
3. Ti-8Al-1Mo-1V, alpha-beta alloy
4. Ti-13V-11Cr-3Al, all-beta alloy

The chemical and physical properties of these alloys reported previously.[2]

2.2 Study of Hydrogen Distribution

To study the distribution of hydrogen in the various titanium alloys selected and its role in stress corrosion cracking by electron microautoradiography technique, the radioactive hydrogen (tritium) was introduced into the alloy samples by two methods: (1) gas adsorption at elevated temperature, and (2) cathodic charging. The results on cathodic charging are described in the second progress report.[2] The results on gas adsorption of tritium at elevated temperatures are described here.

Tritium gas was introduced into each of the four titanium alloys employing a modified Sieverts apparatus designed and fabricated by Astropower Laboratory. The apparatus, as previously described, is comprised of a forepump, two-stage mercury diffusion pump, ion gage, McLeod gage, tritium inlet system, and sample tubes. A mercury cut-off is used to isolate the vacuum manifold from the diffusion pump. The McLeod gage is accurately calibrated and covers the pressure range from 10^{-3} to 1 torr. The ion gage was used only to determine the ultimate vacuum obtainable in the system during initial outgassing and pump down. The tritium inlet system employs a mercury-sealed fritted glass disc valve to admit the tritium to the vacuum manifold. Individual samples 1/4 inch by 1 inch were pickled in an aqueous solution of HNO_3-HF and placed in vertical Vycor tubes which were attached to the Pyrex manifold using graded seals. With the manifold isolated from the vacuum pumps by the mercury cut-off, the total volume of the manifold was determined

by expanding a known pressure of air (approximately 1 torr) from the known volume of the McLeod gage tube to the manifold. The pressure was re- measured — with the McLeod gage — and the system volume calculated from gas law.

In order to charge titanium alloys, the Vycor tubes containing an alloy sample were heated to 725°C ± 10°C, and held at this temperature until a final steady state pressure was attained in the entire system. The specimen tube was then cooled to ambient temperature and the final pressure was measured. The operation was repeated for each alloy until all the samples were charged. The amount of tritium introduced into each alloy is shown in Table I. The accuracy of the measurements by this technique is within 5%.

Before describing results, a brief description of the characteristics of tritium in titanium should be discussed Tritium is a beta emitter with a halflife of 12.26 years. The beta particle has an energy of 0.018 MeV and thus has a maximum penetration in titanium of 1450 angstroms. Thus all tritium deeper in the metal than 1450 angstroms will not be recorded on the emulsion. Furthermore, since a beta particle may emit in any direction, this means that the minimum resolution is 1450 angstroms, i.e., any silver filament observed on the radiograph must be within 1450 angstroms of the actual location of the tritium atom that emitted the beta particle which caused that particular silver filament.

The electron microautoradiographs of titanium alloys charged with tritium at 725°C were prepared as follows:

1. Ten angstroms of chromium were shadowed at 20 degrees. The chromium was placed on the specimen to act as a shadow for the direct carbon replica.
2. 150 angstroms of carbon were deposited onto the titanium for a direct replica of the metal surface.
3. A monolayer of Kodak NTE nuclear track emulsion was then placed on the surface.
4. The specimens were exposed for 16 hours.
5. The emulsion was developed while on the specimen and fixed.
6. The carbon replica and emulsion were removed with nitric acid and hydrofluoric acid.
7. The autoradiograph was rinsed, dried, and examined in the electron microscope.

TABLE I

CONCENTRATION OF TRITIUM IN TITANIUM ALLOYS

Alloy	Concentration (ppm)
Ti-5Al-2.5Sn	48
Ti-6Al-4V	41
Ti-8Al-1Mo-1V	43
Ti-13V-11Cr-3Al	43

2.2.1 Observations on Ti-13V-11Cr-3Al Alloy

Tritium was evenly distributed throughout the lattice of this all-beta alloy. There was no apparent concentration at boundaries. Figure 1 is a microautoradiograph showing distribution of tritium in two different beta grains of Ti-13V-11Cr-3Al alloy.

The efficiency of the NTE emulsion was determined using this alloy because of the uniform distribution of tritium in the beta matrix. Using the maximum penetration of beta particles in titanium as 1450 Å, the efficiency of the emulsion was estimated as 40 to 50%.

2.2.2 Observations on Ti-8Al-1Mo-1V and Ti-6Al-4V Alloys

The tritium distribution in Ti-8Al-1Mo-1V and Ti-6Al-4V alpha-beta alloys was very similar. Most of the tritium was concentrated in the beta phase of these two alloys. Figures 2 and 3 show the results of this experiment.

2.2.3 Observations on Ti-5Al-2.5Sn Alloy

Charging of 48 ppm of tritium gas at 725°C and subsequent air quenching produced extensive cracking in this alpha alloy as shown in Figure 4. Examination of the microstructure of metal in the region of the crack showed that the fracture was intergranular. Optical microscope observation showed precipitates at alpha grain boundaries following tritium charging. A microautoradiograph of this alloy showed a uniform distribution of tritium in the alpha grains, but a high concentration of tritium at the precipitates. Figure 5 shows the results of this experiment.

2.3 Stress Corrosion Cracking Tests

The process of stress corrosion cracking in alloys usually commences as a pitting attack rather than as uniform corrosion, and in the general case, stress corrosion does not initiate until a pit grows deep enough to act as a stress raiser. By inserting a fatigue crack in the specimen before commencing the test, stress corrosion can be caused to initiate immediately upon application of sufficient stress. The stress at the root of a crack can be described quantitatively by the stress intensity factor, K. The stress intensity factor at the point of crack instability is designated K_c. The advantages of

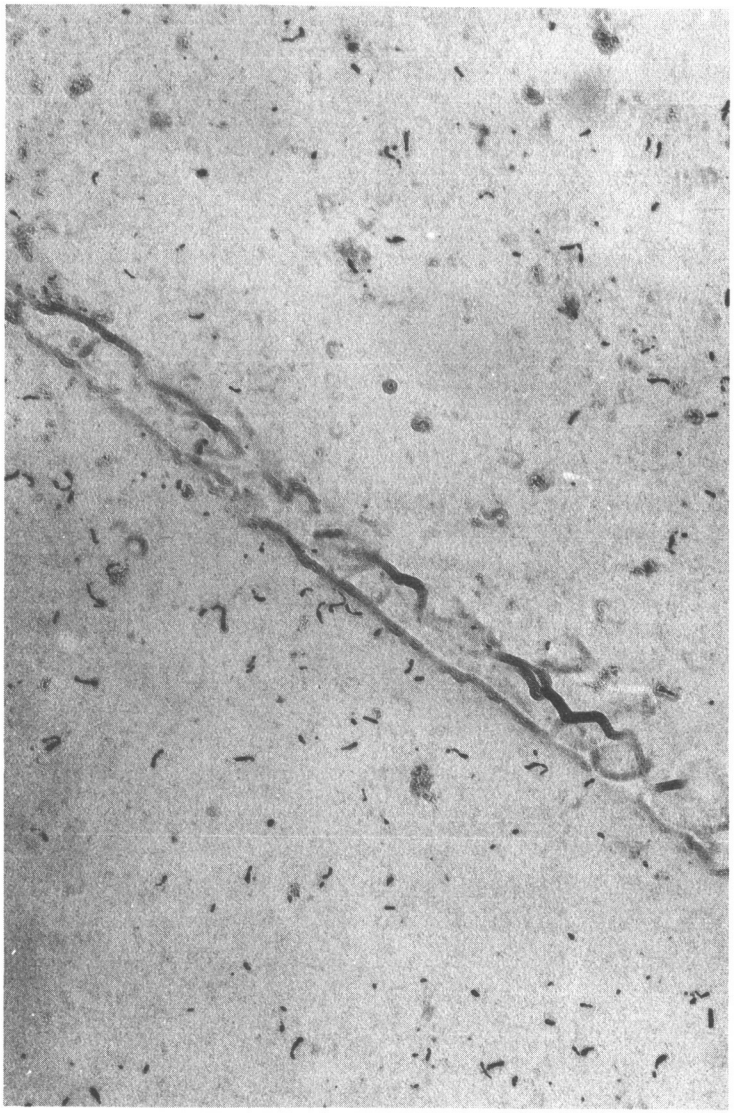

C2921

Figure 1. Microautoradiograph of Tritium in Ti-3Al-13V-11Cr. Magnification 20,000X.

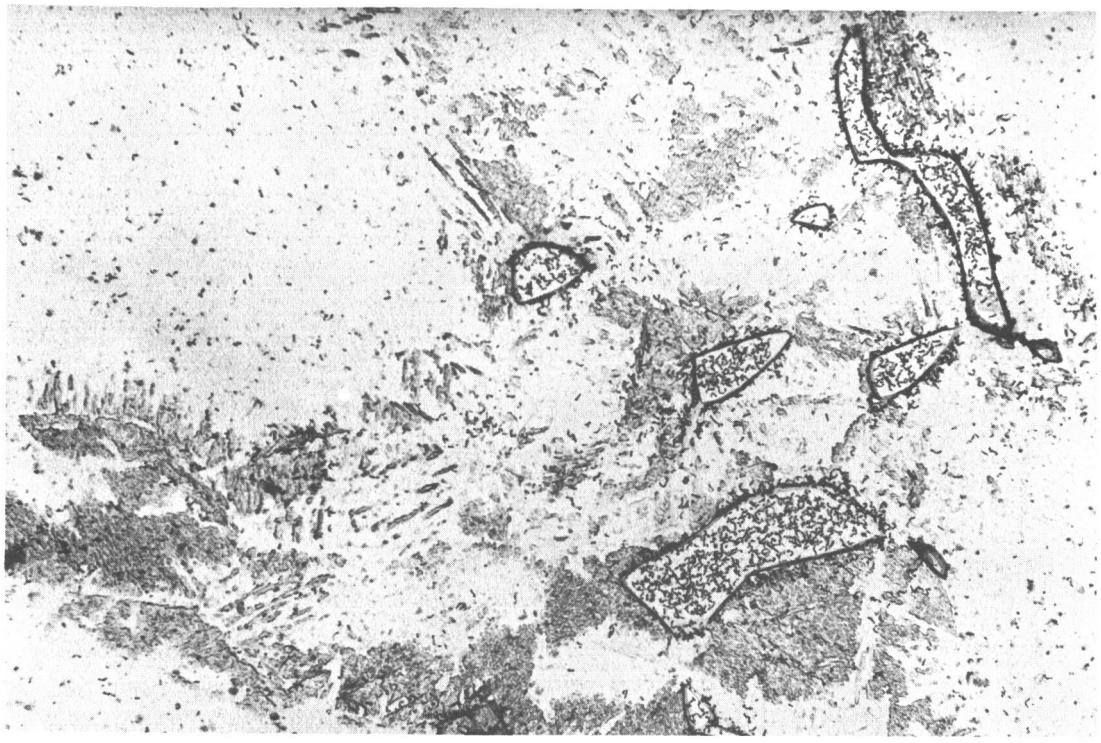

(a)

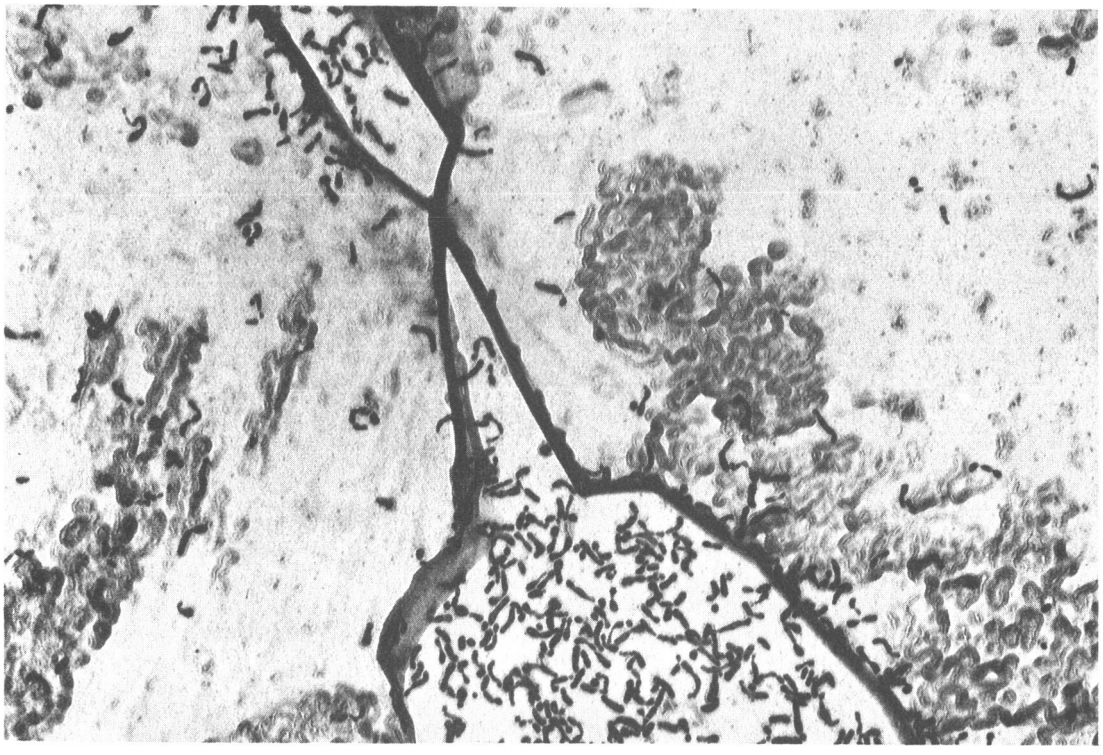

(b)

(a) 8,000X
(b) 30,000X

Figure 2. Microautoradiographs of Tritium in Ti-8Al-1Mo-1V. Tritium is concentrated in beta phase.

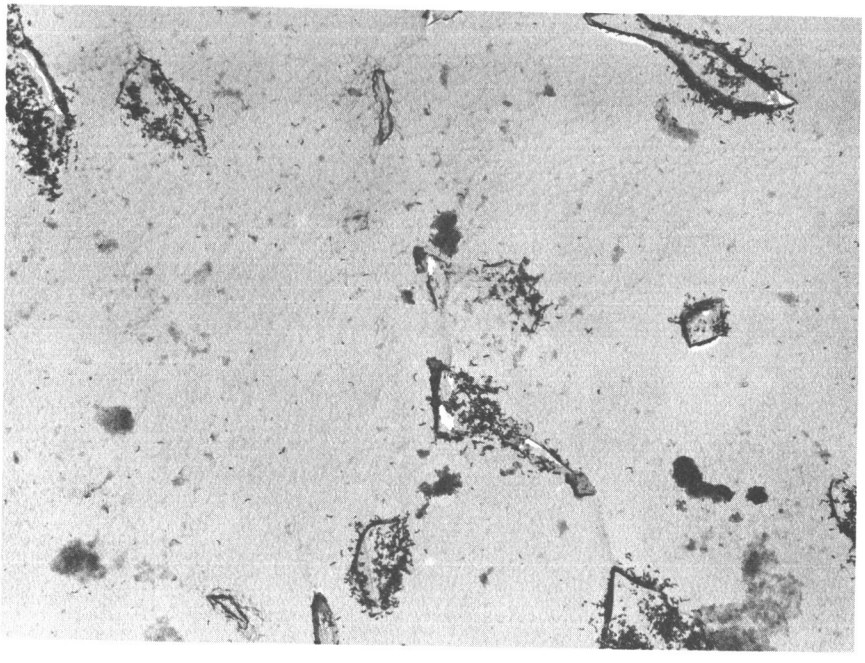

(a)

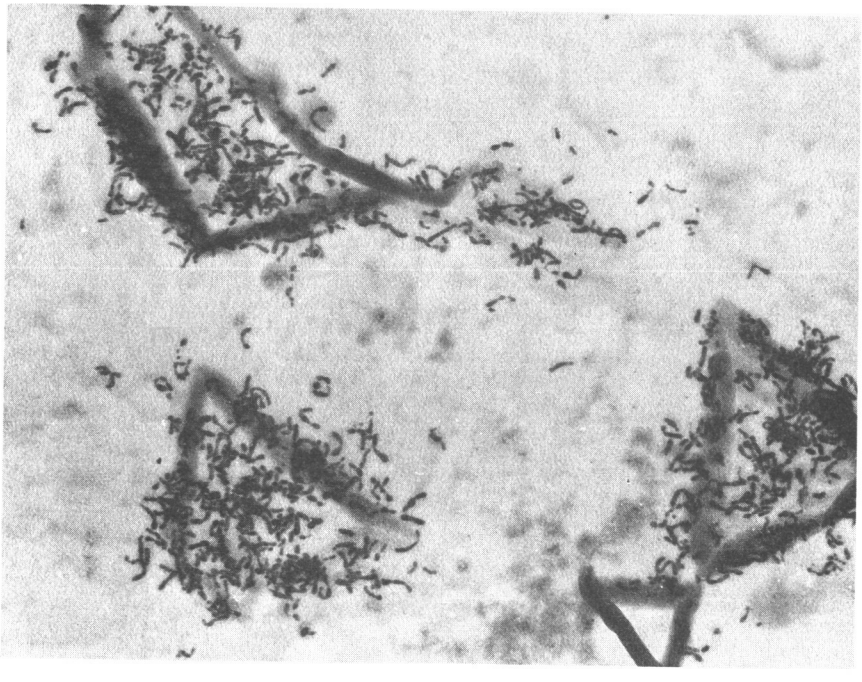

02923

(b)

(a) 4,500X
(b) 15,500X

Figure 3. Microautoradiograph of Tritium in Ti-6Al-4V. Tritium is concentrated in the beta phase.

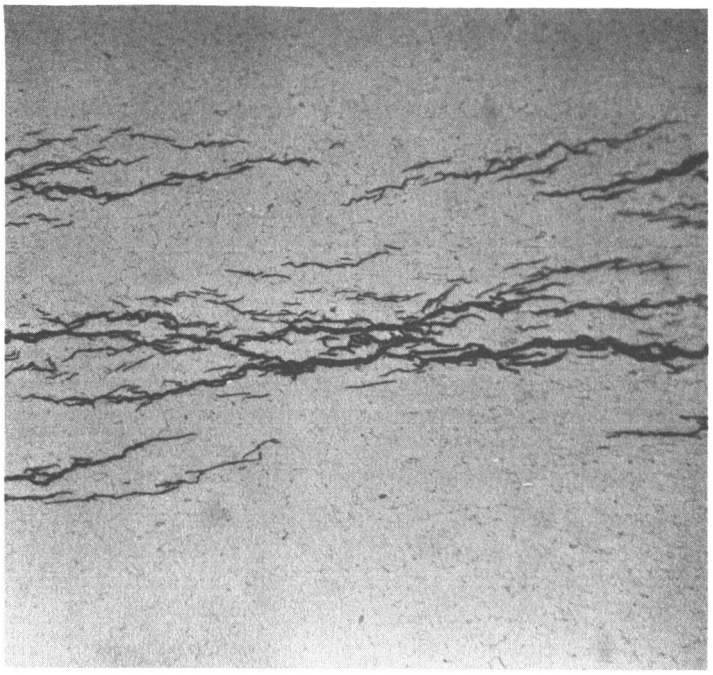

02924

Figure 4. Development of Cracks in Ti-5Al-2.5Sn Due to Charging of 48 ppm Tritium at 725°C. Magnification 175X.

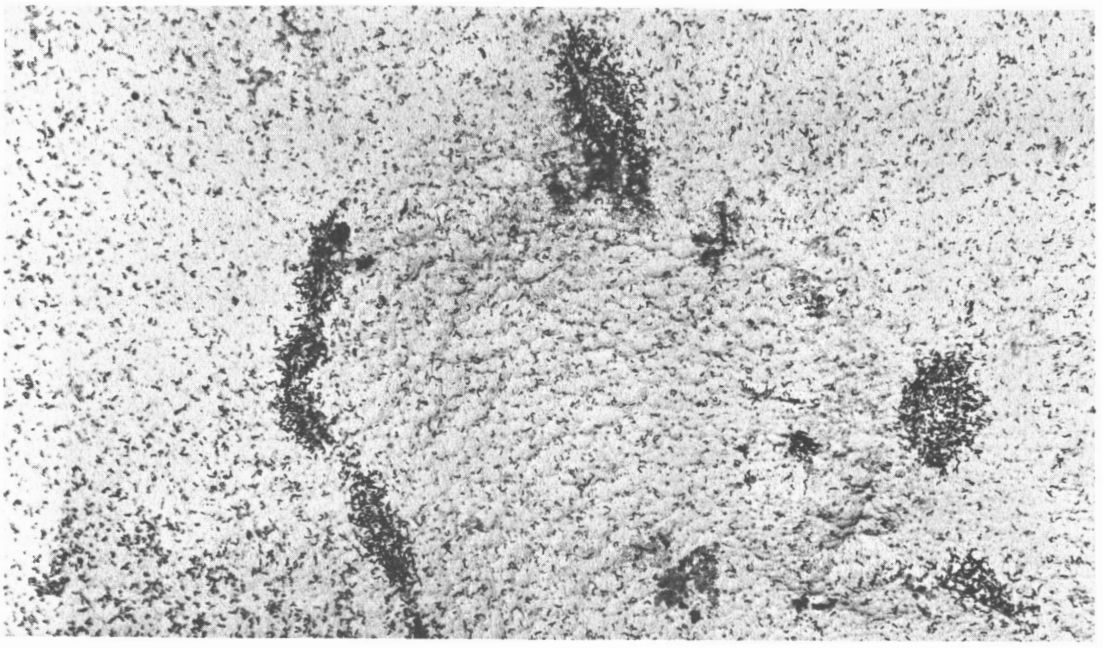

(a)

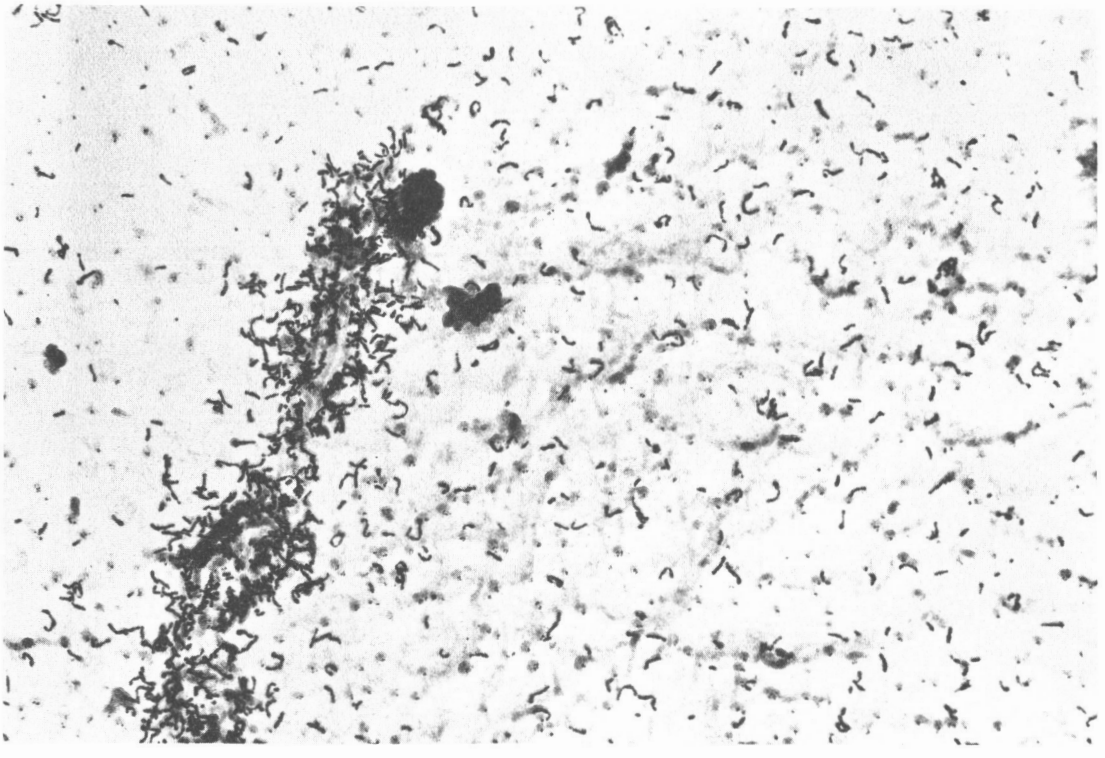

(b)

C2925

(a) 6,000X
(b) 30,000X

Figure 5. Microautoradiograph of Tritium in Ti-5Al-2.5Sn. Tritium is concentrated at beta precipitated in alpha grain boundaries.

using a fatigue cracked specimen for testing for stress corrosion susceptibility are:

1. One can greatly shorten the time for testing.
2. One can test for stress corrosion cracking in alloys which do not pit.
3. One can describe quantitatively the state of stress at the initiation of stress corrosion cracking whereas this would not be possible with a stress raiser in the form of an irregular pit.

Stress corrosion tests have been performed for the selected titanium alloys in 3% NaCl solution and distilled water at ambient temperature. The single-edge notch plate configuration previously described[3] was used for these tests. The load was increased in increments of 40 lb starting at 1000 lb. The load was held for five minutes at each load level. The fatigue crack was observed with a stereo microscope and the time of initiation of crack extension was measured with a stopwatch. The stress intensity factor, at crack instability, K_c, was calculated using the following equation:[4]

$$K_c^2 = \frac{P^2}{B^2} \quad \frac{1}{W} \left[7.59 \left(\frac{a}{w}\right) - 32 \left(\frac{a}{w}\right)^2 + 117 \left(\frac{a}{w}\right)^3 / 1 - v^2 \right] \qquad (1)$$

where

P = load
B = thickness
A = crack length
w = width of specimen
v = Poissons ratio

The above procedure employs static loading and it is not possible to measure the critical stress intensity parameter, K_{IC}, by this technique. Step loading usually produces small different K_{ISCC} than loading several specimens to different K_c values. However, in these experiments the purpose is to study crack propagation and the method of loading will not affect the mechanism of propagation.

The initial fatigue crack length, a, in equation (1) was measured with a low power microscope following fracture of the specimen, and was used

to calculate K_c. The stress intensity factor, K_c, to propagate a crack in air, in a 3% salt solution and in distilled water for the titanium alloys tested, is summarized in Table II.

Included in this table are a few specimens of Ti-5Al-2.5Sn which were vacuum annealed (10^{-6} torr) at 1400°F for 24 hours and 42 hours to remove the residual hydrogen. A hydrogen chemical analysis for 24 hour vacuum anneal showed 39 ppm and for 42 hour vacuum aneal showed 30 ppm. A hydrogen chemical analysis of as-received Ti-5Al-2.5Sn showed 61 ppm hydrogen.

The reduction of stress intensity factor, K_c, by 3% salt solution and by distilled water at ambient temperature when compared with values obtained in argon or air showed that all-alpha alloy Ti-5Al-2.5Sn and alpha-beta alloys Ti-8Al-1Mo-1V and Ti-6Al-4V were susceptible to stress corrosion cracking in these environments. The sodium chloride environment lowered the stress intensity factor, K_c, to a much lower value than distilled water. The beta alloy, Ti-13V-11Cr-3Al did not show susceptibility to stress corrosion cracking at ambient temperature in these environments.

The minimum value of the stress factor to cause stress corrosion cracking has been designated by Brown[5] as K_{ISCC}. This threshold value can be found by plotting stress intensity factor, K_c, versus time-to-fracture. Figures 6 and 7 show results obtained for Ti-8Al-1Mo-1V and Ti-5Al-2.5Sn in 3% salt and distilled water at ambient temperature. Two significant differences were observed between stress corrosion cracking in distilled water and 3% salt solution: (1) a higher stress intensity was required to initiate crack propagation in distilled water than in 3% NaCl solution and (2) the crack propagation was much faster in salt solution than in distilled water.

2.4 Electron Fractography of Crack Propagation

In order to define the mode of stress-corrosion crack propagation, the fracture faces and profiles of titanium alloy samples were examined by replica techniques. The method of replication consisted of the two-stage carbon-plastic method. A 5% parlodion in amyl acetate was applied on the fracture face directly, or after etching. The parlodion was allowed to harden in place, stripped

TABLE II

STRESS INTENSITY FACTOR, K_c, FOR Ti-8Al-1Mo-1V, Ti-6Al-4V, Ti-13V-11Cr-3Al AND Ti-5Al-2.5Sn IN 3% SALT SOLUTION AND DISTILLED WATER

Alloy	Environment	K_c (Ksi$\sqrt{in}$)	Time to Fracture (min.)
Ti-8Al-1Mo-1V	Argon	43.7	—
"	Argon	44.8	—
"	3% Salt	28	0.6
"	3% Salt	25.2	1.0
"	3% Salt	23.0	1.0
"	3% Salt	18.5	1.5
"	Distilled Water	36.6	1.1
"	Distilled Water	30.4	2.2
"	Distilled Water	24	4.0
"	Distilled Water	22	6.0
Ti-5Al-2.5Sn	Air	129	2.5
"	3% Salt	58.0	2.0
"	3% Salt	48.3	1.0
"	3% Salt	33	2.5
"	3% Salt	40	1.2
"	3% Salt	34.3	2.5
"	3% Salt	33	2.5
"	Distilled Water	95	4.6
"	Distilled Water	82.5	3.0
"	Distilled Water	81	4.0
"	Distilled Water	71	4.0
"	Distilled Water	68.5	4.7
"	Distilled Water	64	6.0
Ti-5Al-2.5Sn (Vacuum Heat Treatment 24 hr)	Air	120	—
"	3% Salt	27	—
" 42 hr	Air	120	—
"	3% Salt	30	2.5
Ti-6Al-4V	Air	75.5	—
"	Air	75.5	—
"	3% Salt	57	0.5
"	3% Salt	48	2.0
"	3% Salt	45	2.0
"	3% Salt	44	2.0
"	3% Salt	43	3.0

(Continued)

TABLE II (CONTINUED)

STRESS INTENSITY FACTOR, K_c, FOR Ti-8Al-1Mo-1V, Ti-6Al-4V, Ti-13V-11Cr-3Al AND Ti-5Al-2.5Sn IN 3% SALT SOLUTION AND DISTILLED WATER

Alloy	Environment	K_c (Ksi$\sqrt{in}$)	Time to Fracture (min.)
Ti-6Al-4V	3% Salt	42	3.0
"	Distilled Water	71.5	2.7
"	Distilled Water	71.5	8.0
Ti-13V-11Cr-3Al	Air	101	—
"	3% Salt	95.2	0.34
"	3% Salt	90	1.0
"	3% Salt	85.2	4.0
"	Distilled Water	97.4	6.0
"	Distilled Water	92	16.0

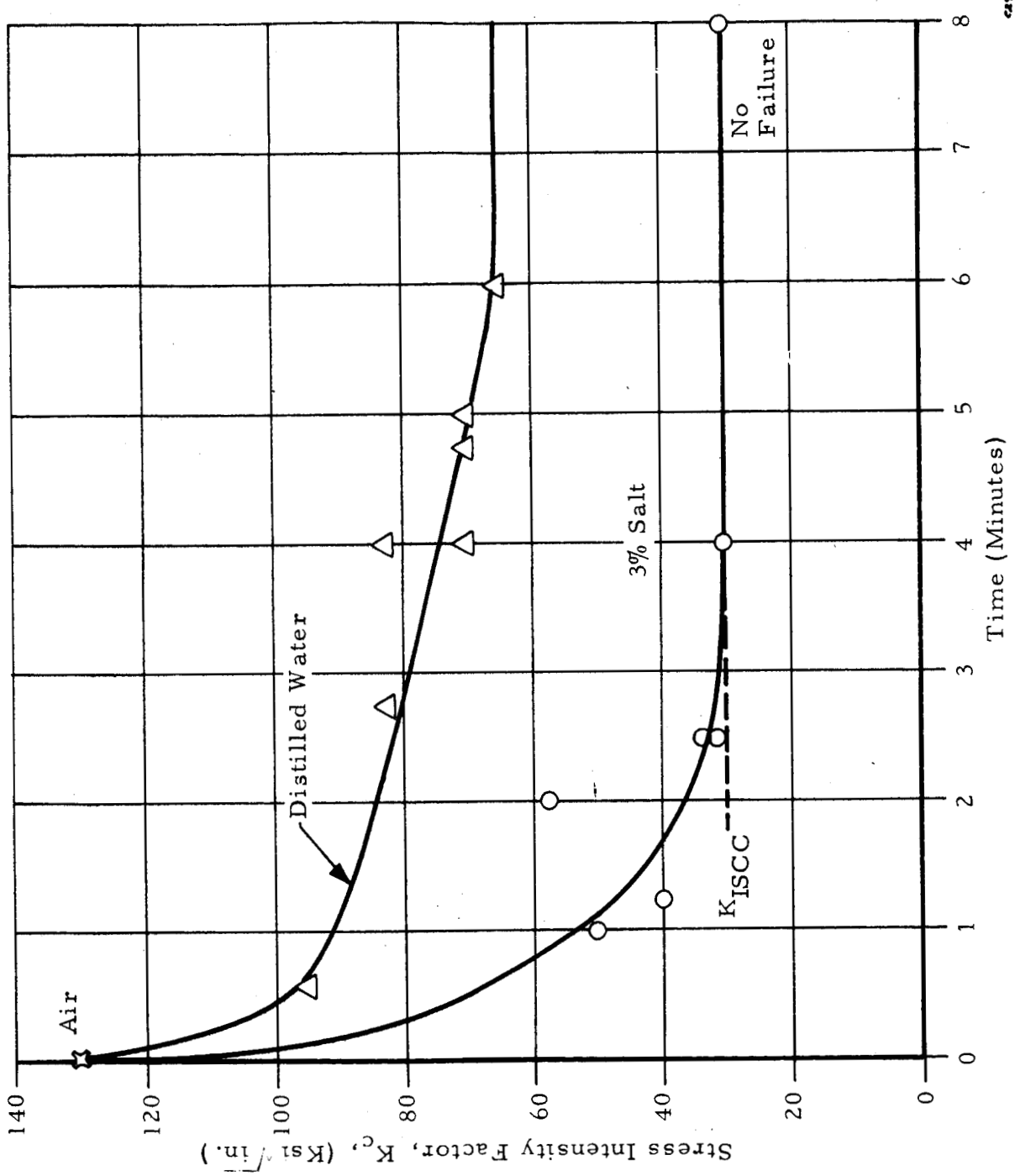

Figure 6. Effect of Initial Stress Intensity on Time-To-Fracture for Ti-5Al-2.5Sn at Ambient Temperature

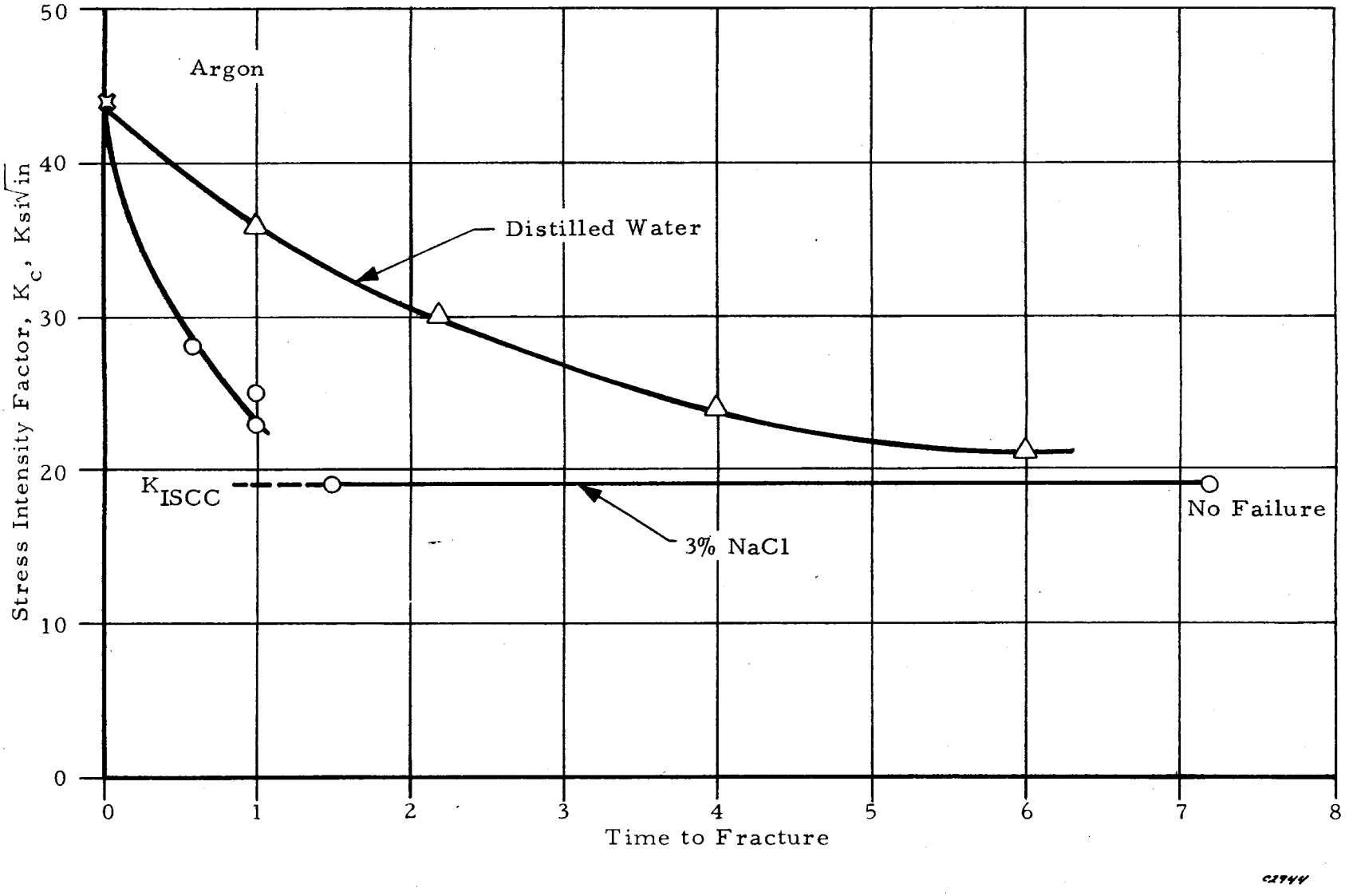

Figure 7. Effect of Initial Stress Intensity on Time-to-Fracture for Ti-8Al-1Mo-1Ti at Ambient Temperature

from the surface, deposited with carbon at a 90 degree angle, and shadowed with chrome at a 45 degree angle. The parlodion was then dissolved in acetone leaving the final Cr-C replica, which was carefully placed on electron microscope grids.

The profile of fracture faces was prepared by cleaning the test sample in distilled water, plating the fracture surface by immersion in a nickel plating bath, microsectioning and replicating the polished and etched section. The electroless nickel bath was a commercial Enthone type 410B solution. The bath acidity was adjusted to pH 4.3 to 4.5, and the bath temperature was 190 to 195°F. The plate thickness produced was 0.0025 inch. The replication of the polished and etched surface was the two-stage carbon-plastic method similar to direct replica. The 5% parlodion in amyl acetate was applied to 200 mesh copper grids placed at the desired crack zone. After drying, the grid and plastic were stripped from the mount with scotch tape, the grids were removed, the negative replica deposited with carbon, shadowed with chromium, and the parlodion dissolved in acetone leaving the final Cr-C replica.

Figure 8 shows a two-stage Cr-C replica of an all-beta type alloy (Ti-13V-11Cr-3Al) notched specimen failed under static stress in air. Similar microstructure was noted in samples fractured in distilled water and salt solution. The fracture face is virtually all dimpled structure, indicative of ductile failure.

Figure 9 shows the fracture face of an alpha-beta alloy, Ti-6Al-4V, fractured in stress cracking in air. The fracture face exhibits ductile dimpled structure virtually throughout the surface, with some intergranular fracture facets. Figure 10 is the fractured face in stress corrosion in salt solution. The surface exhibits mixtures of cleavage and ductile regions. The cleavage areas (arrow A) are identified by river markings. The ductile areas (arrow B) are characterized by large dimples with deformation markings or serpentine glide and ripples on the surface.[6]

Attempts have been made to relate the cleavage areas to microstructure by etching the fracture surface before making the fractograph. This method has been successful in studying the hot salt stress corrosion of titanium alloys.[7] During etching many of the fracture features are removed. Figure 11

shows that with sufficient etching beta is revealed (compare Figure 11 with an unetched fracture such as Figure 10). In these experiments we have not yet taken fractographs from the same area before and after etching. However, Figure 11 does suggest one significant result. Arrow A points to a beta phase which exhibits cleavage markings.

Profile cross sections of the fracture edge were made of the Ti-6Al-4V alloy failed in air and in salt solution. The fracture in air (Figure 12) indicated transgranular ductile rupture and distortion of alpha. The fracture in salt solution (Figure 13) indicated that the crack path appears to follow alpha-beta phase boundary by cleavage, and rupture is possibly not taking place through the beta phase. This observation is contrary to the results reported by Beck[8] that failure in Ti-8Al-1Mo-1V alloy under SCC condition occurs by apparent cleavage in the alpha phase and ductile failure of the beta phase. It is apparent that hydrogen segregation in the beta phase as demonstrated in Section 2.2, might be associated with the type of cleavage failure of the alpha-beta phase boundary described here. Further work along these lines will be of great benefit in clarifying the nature of cleavage.

The fracture faces of the Ti-8Al-1Mo-1V alloy failed in distilled water and salt solution exhibited similar morphology to the Ti-6Al-4V alloy. Figures 14 and 15 show mixtures of local cleavage and ductile rupture areas. There was also some evidence of intergranular fracture regions for this alloy.

The fracture surface of the alpha type alloy, Ti-5Al-2.5Sn, failed in air, is shown in Figure 16. The fracture face predominantly shows dimple rupture (arrow A), and some evidence of (serpentine) glide and deformation markings (arrow B), characteristic of ductile fracture.[6] The microfractograph of specimens failed in distilled water showed predominantly ductile rupture with some local cleavage areas (Figure 17). The salt water stress corrosion fracture face exhibited much larger areas of cleavage distributed throughout the surface, as illustrated in Figure 18.

Also examined were profile cross sections of the alpha alloy, Ti-5Al-2.5Sn, failed in air and salt solution. Figure 19 shows ductile transgranular fracture in air with distorted alpha grains. There was some indication that the fracture path followed along alpha grain boundaries where

62928

Figure 8. Electron Fractograph of Beta Alloy Ti-13V-11Cr-3Al Fractured in Air. Note dimple rupture. Magnification 7,500X.

Figure 9. Electron Fractograph of an Alpha-Beta Alloy Ti-6Al-4V Fractured in Air. Note dimple rupture. Magnification 7,500X.

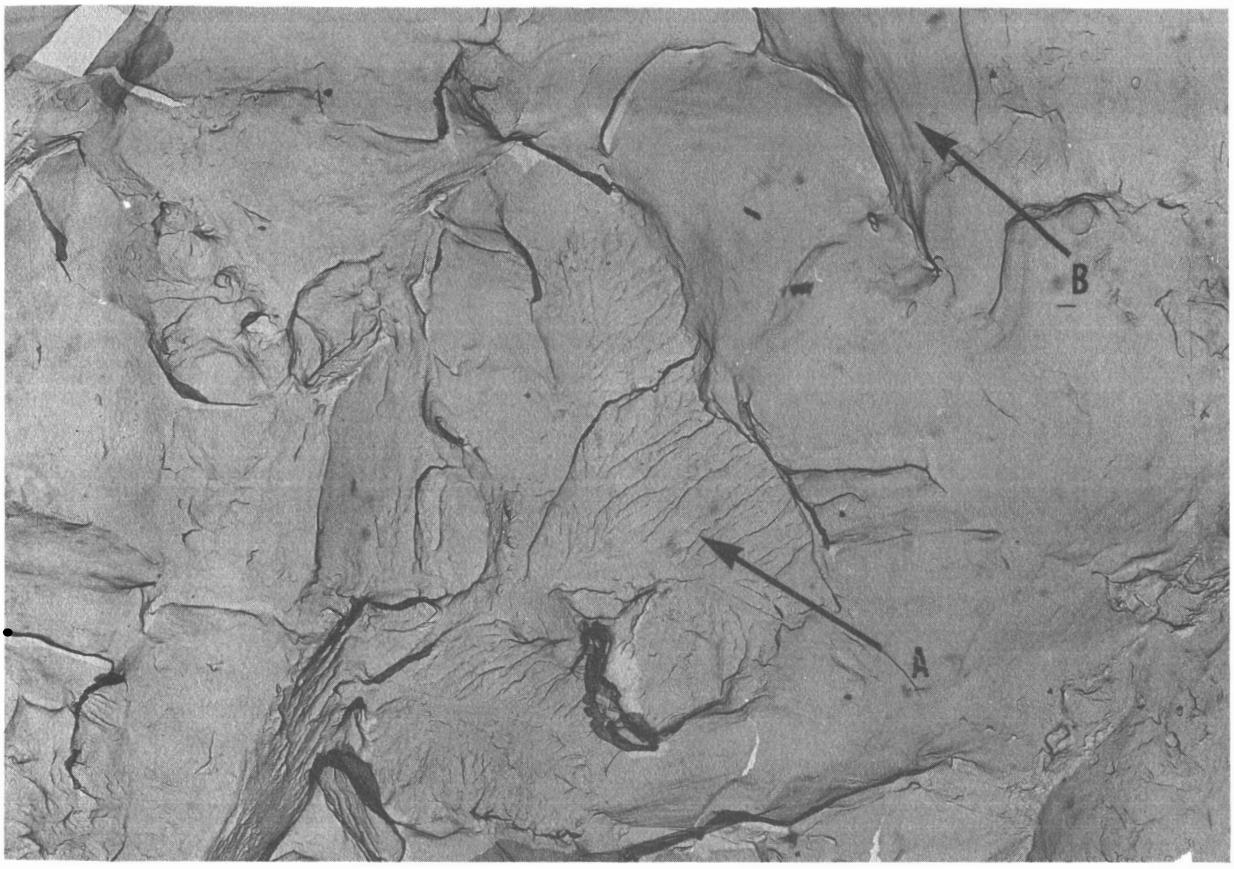

Figure 10. Electron Fractograph of Stress Corrosion Region of Ti-6Al-4V Fractured in 3% Salt Solution. Fractograph shows a mixture of cleavage (Arrow A) and ductile failure (Arrow B). Magnification 7,500X.

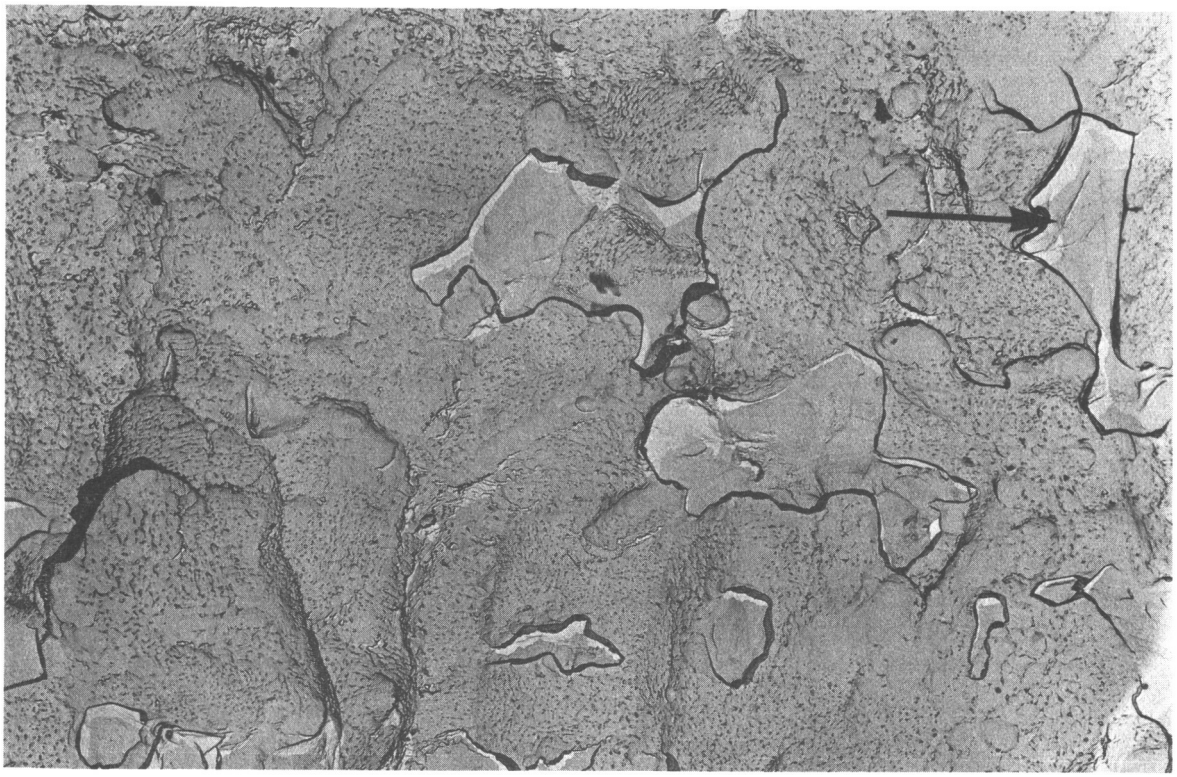

c2929

Figure 11. Electron Fractograph of Stress Corrosion Region of Ti-6Al-4V Fractured in 3% Salt Solution. Fracture has been etched for 15 seconds in HF-HNO_3-H_2O solution. Arrow points to beta phase exhibiting cleavage markings. Magnification 7,500X.

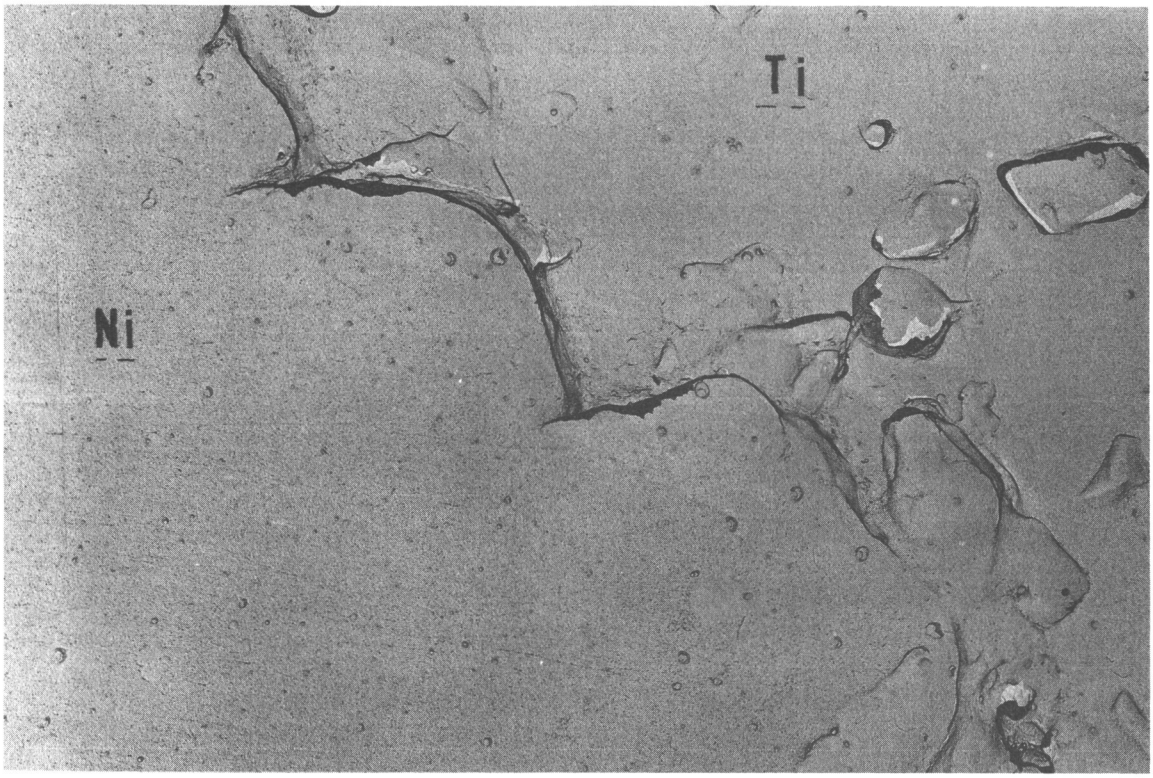

02930

Figure 12. Profile of Fracture Edge of Ti-6Al-4V Fractured in Air. Micrograph shows transgranular ductile rupture. Magnification 7,500X.

Figure 13. Profile of Fracture Edge from Stress Corrosion Region of Ti-6Al-4V Fractured in 3% NaCl Solution. Fracture propagated along an alpha-beta boundary by cleavage (Arrows). Magnification 7,500X.

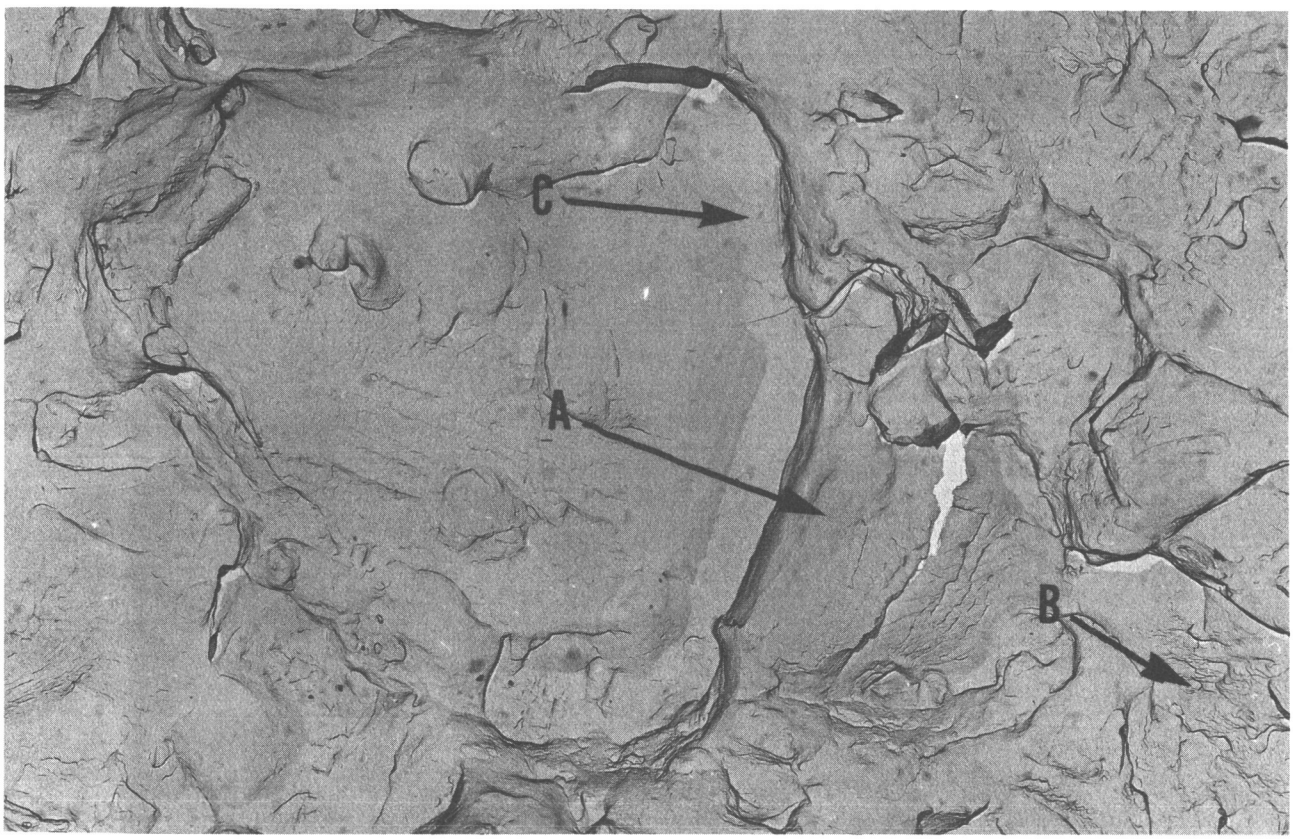

C2932

Figure 14. Electron Fractograph from Stress Corrosion Region of Ti-8Al-1Mo-1V Fractured in 3% Salt Solution. Fractograph shows ductile rupture (Arrow A), cleavage (Arrow B) and evidence of intergranular fracture (Arrow C). Magnification 7,500X.

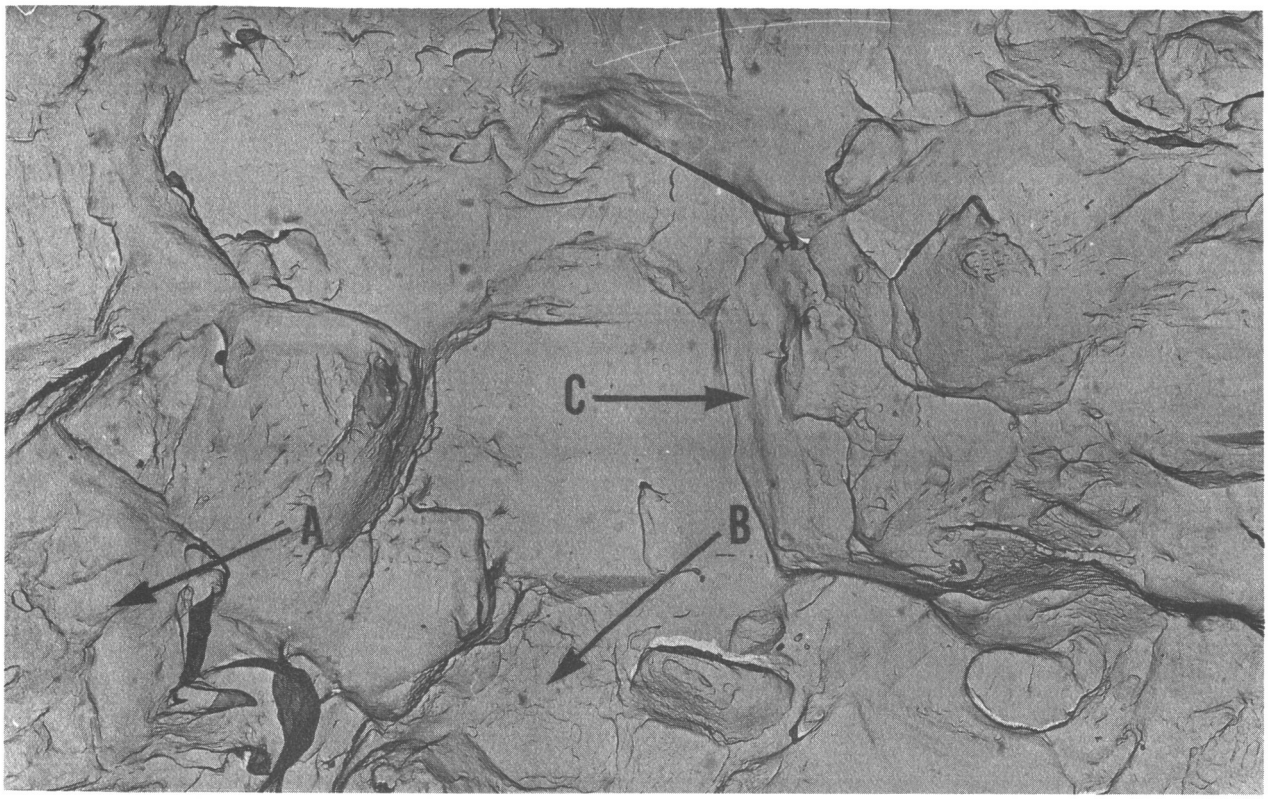

C4933

Figure 15. Electron Fractograph from Stress Corrosion Region of Ti-8Al-1Mo-1V Fractured in Distilled Water. Fractograph shows ductile rupture (Arrow A), cleavage (Arrow B), and evidence of intergranular fracture (Arrow C). Magnification 7,500X.

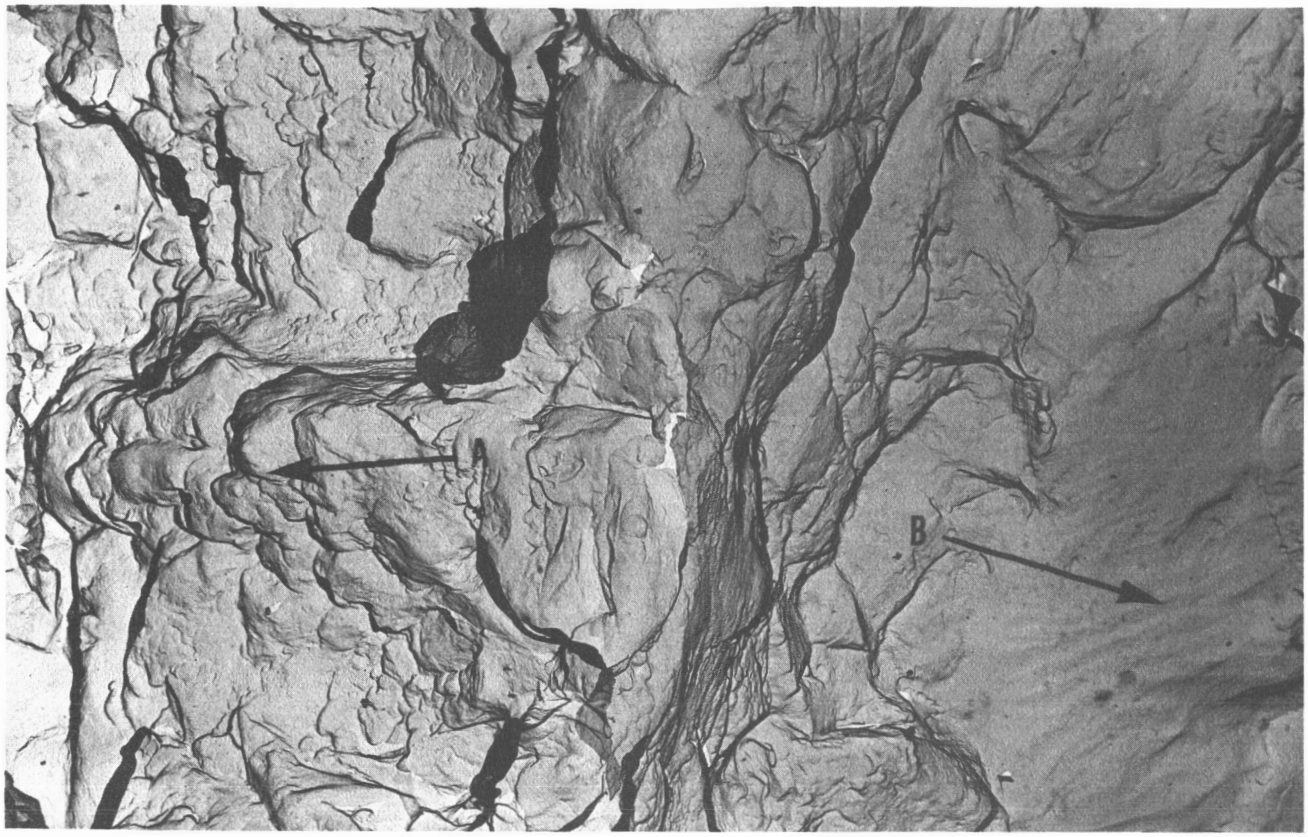

62934

Figure 16. Electron Fractograph of Air Fractured Surface of Ti-5Al-2.5Sn. Fractograph shows dimple rupture (Arrow A), and glide characteristic of ductile fracture (Arrow B). Magnification 7,500X.

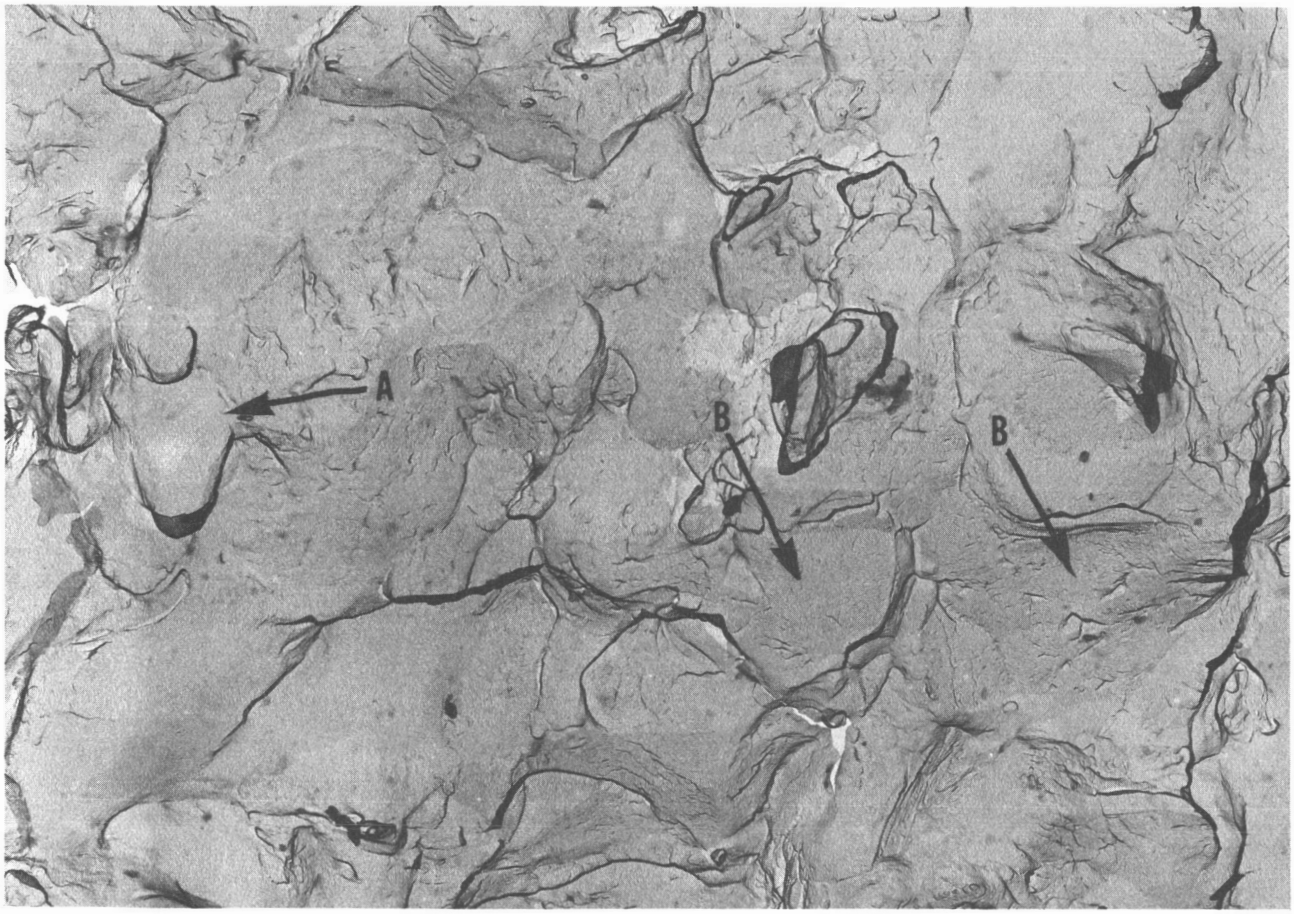

cZ935

Figure 17. Electron Fractograph from Stress Corrosion Region of Ti-5Al-2.5Sn Fractured in Distilled Water. Most of the fracture exhibits ductile failure (Arrow A) in its local cleavage areas distributed throughout (Arrows B). Magnification 7,500X.

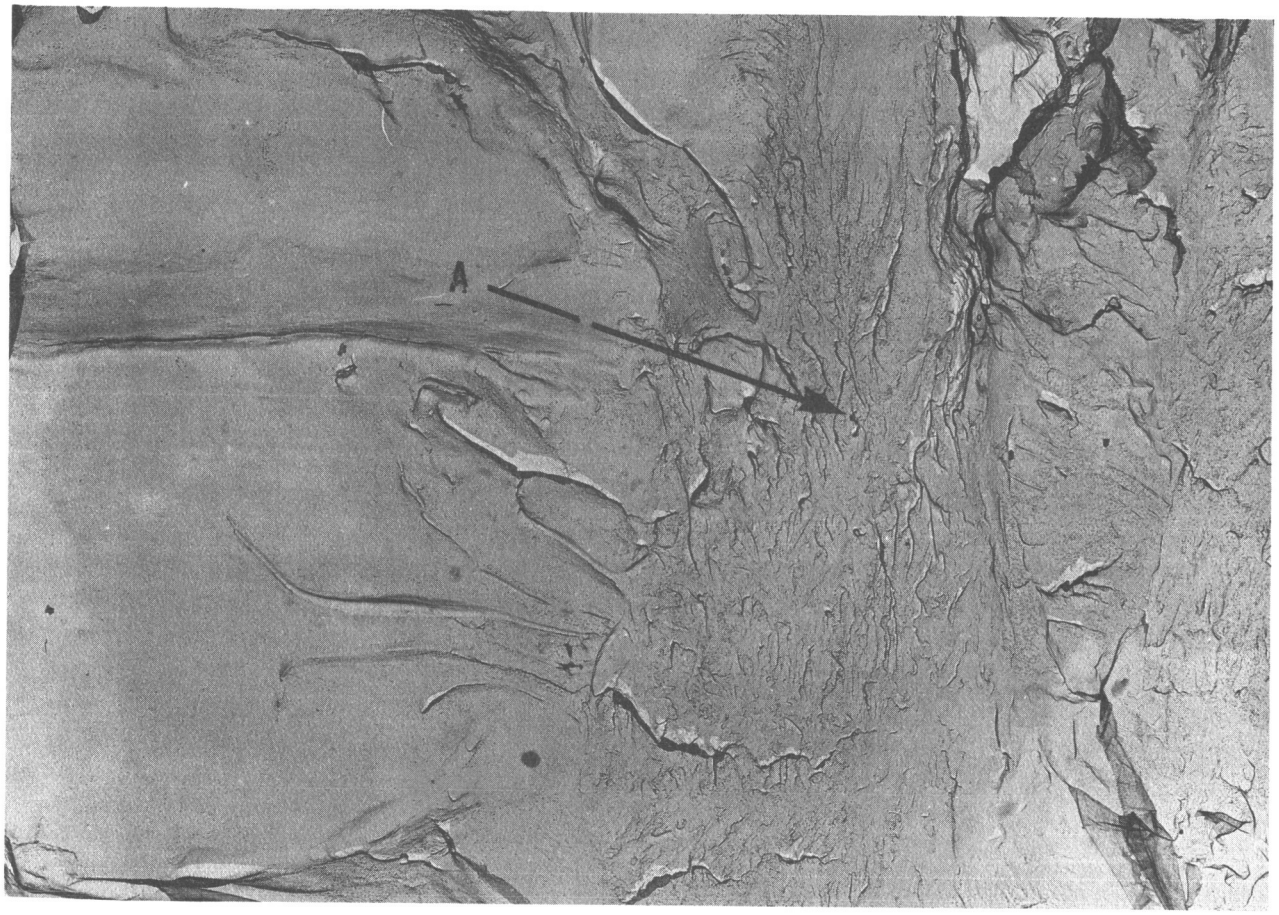

C2936

Figure 18. Electron Fractograph from Stress Corrosion Region of Ti-5Al-2.5Sn Fractured in 3% NaCl. Fractograph shows cleavage area (Arrow A). Most of the fracture exhibits ductile failure with these local cleavage areas distributed throughout. Magnification 7,500X.

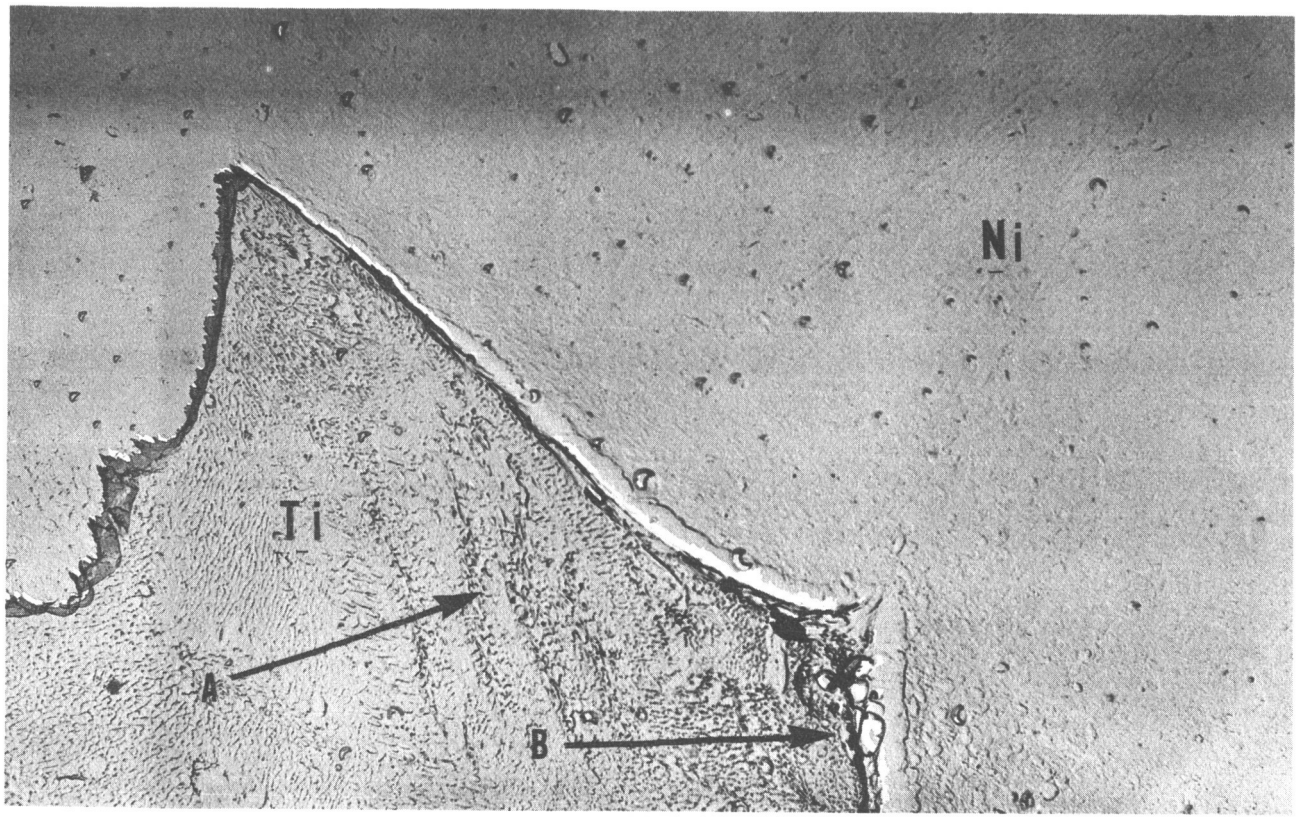

C2937

Figure 19. Profile of Fracture Edge of Ti-5Al-2.5Sn Fractured in Air. Arrow A shows deformed region of alpha, and Arrow B shows failure along an alpha-beta interface. Magnification 7,500X.

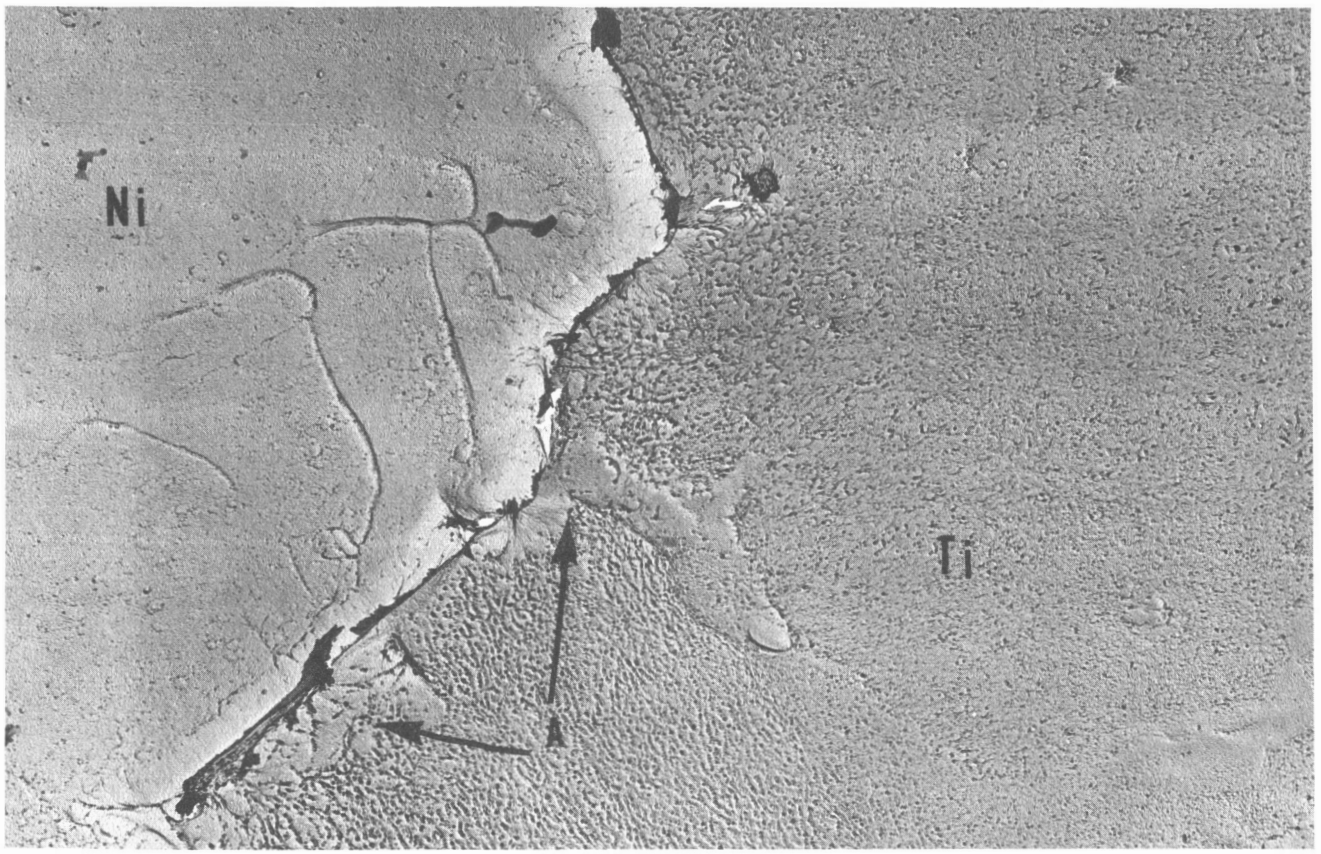

©2938

Figure 20. Profile of Fracture Edge in Stress Corrosion Region of Ti-5Al-2.5Sn Fractured in 3% NaCl Solution. In this region (Arrows A), fracture propagated along an alpha-beta interface. Beta particles were precipitated in alpha grain boundaries. Magnification 7,500X.

retained beta was formed. Specimens fractured in the salt solution exhibited less distortion of the alpha phase, and cleavage along the alpha-beta boundaries (Figure 20). The cleavage areas from salt solution fracture are considerably larger in size than the retained beta phase observed in the profiles; however, in distilled water the cleavage areas are comparable in size with the retained beta. The segregation of hydrogen in these local regions appears to play a role in their cleavage behavior. Further work with alloys at different hydrogen content may elucidate the role of local cleavage regions in SCC.

2.5 Electrochemical Measurements

To elucidate the effect of the hydrogen content of titanium alloys on the electrochemical behavior, further polarization experiments were conducted with the alpha type alloy, Ti-5Al-2.5Sn, in oxygenated 3% NaCl solution at pH 6.5. Two types of alloy specimens were employed: (1) as received with 61 ppm hydrogen, and (2) vacuum annealed (10^{-6} torr) at 1400°F for 24 hours with 39 ppm hydrogen.

An examination of the polarization curves (Figures 21 and 22) indicated the following:

1. The rest potential of the alloy in unstressed condition was shifted in the electropositive (noble) direction with increased hydrogen content (from -0.4V for 39 ppm, to -0.2V for 61 ppm), and the anodic branch in the passive region was reduced in width.

2. Stressing to 80% of yield stress did not change the polarization curve in the passive region of the alloy with low hydrogen, but lowered the corrosion current (from about 0.02 to 0.003 ma/cm^2) in the passive region of the alloy with high hydrogen. Cathodic polarization branches were essentially the same. The anodic polarization branches in the transpassive region differed greatly, with the hydrogen content suggesting other complicated side reactions.

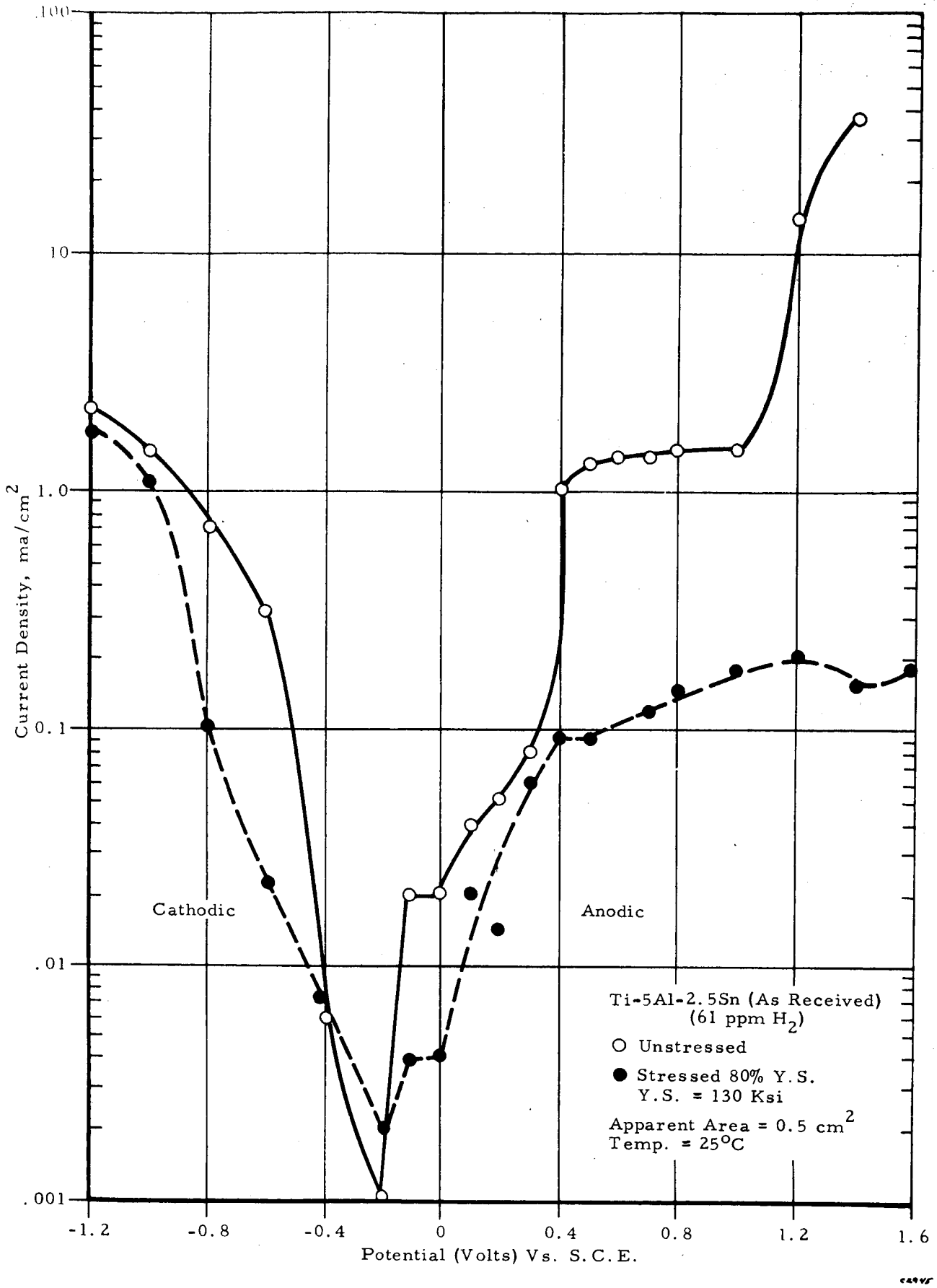

Figure 21. Polarization Curves of Ti-5Al-2.5Sn Alloy in Oxygenated 3% NaCl, pH 6.5

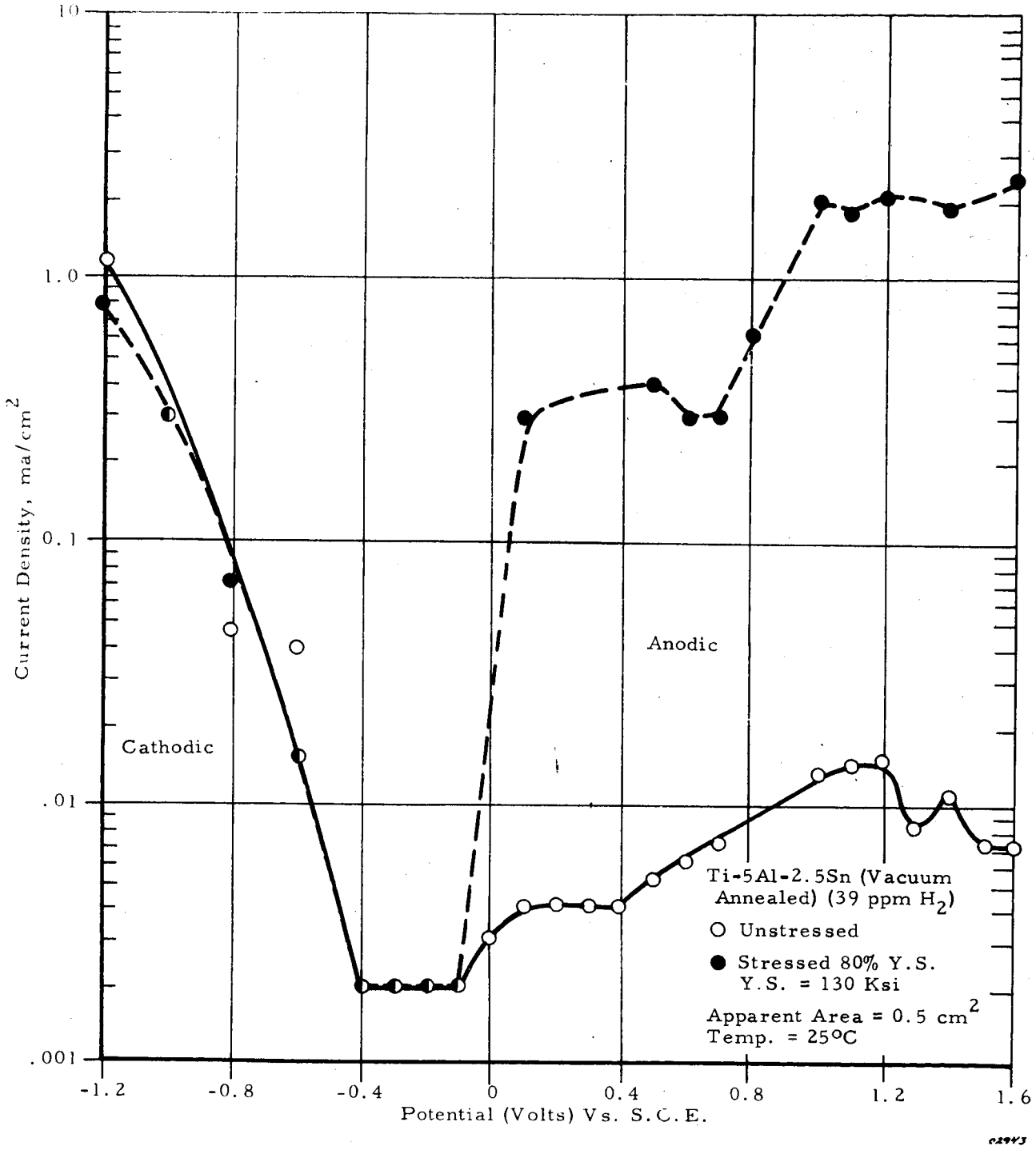

Figure 22. Polarization Curves of Vacuum Annealed Ti-5Al-2.5Sn Alloy in Oxygenated 3% NaCl, pH 6.5

3.0 CONCLUSIONS

The following conclusions can be made on the work accomplished during the third quarter.

Electron microautoradiography work clearly demonstrated that hydrogen gas in quantities less than 50 ppm (in radiotracer form H^3) introduced into titanium alloys is preferentially segregated in beta phase in alpha-beta type alloys, or alpha grain boundaries in alpha alloys, and is uniformly dispersed in all beta type alloys.

Precracked notched alpha type Ti-5Al-2.5Sn and duplex annealed alpha-beta type Ti-8Al-1Mo-1V, and Ti-6Al-9V alloys exhibited lower resistance to SCC in aqueous salt solutions whereas beta type Ti-13V-11Cr-3Al did not exhibit a noticeable effect.

All beta type alloys exhibit ductile dimple microstructure in fracturing in air and salt solutions. Alpha-beta and alpha type alloys exhibit mixtures of ductile dimple and brittle cleavage areas in fracture faces. The cleavage areas are much larger in stress cracking in aqueous salt solutions, compared to air fracturing.

The stress corrosion crack paths propagate, in general, transgranularly through alpha grains but follow by cleavage to the alpha-beta phase boundaries. The segregation of hydrogen in the beta phase appears to play a role in this brittle behavior of the beta regions.

The reduction of the original hydrogen content in the alpha alloy Ti-5Al-2.5Sn from 60-70 to 30-40 ppm did not seem to affect drastically the stress intensity parameter in aqueous salt solutions, as observed by Howe[9] with alpha-beta alloys. The results are preliminary and some electrochemical changes appear to occur, as illustrated by the lowering of corrosion current in the passive region by stressing alloys with increased hydrogen content.

4.0 FUTURE WORK

Electron microautoradiography studies will be carried out with tritiated alloy samples to evaluate the effect of stress on hydrogen distribution.

More electron fractography studies will be conducted with alpha-beta alloys to demonstrate the mode of propagation of the crack path.

The sites of local dissolution of the titanium alloy matrix will be evaluated by transmission electron microscopy. Thin foils of titanium alloys suitable for transmission of an electron beam will be prepared. The foils will be examined, and then dipped in distilled water or salt solution and re-examined to evaluate preferential attack.

Polarization measurements will be conducted with alpha-beta alloys to clarify the effect of stress on reaction rates.

REFERENCES

1. Gilpin, C. B., S. M. Toy, and N. A. Tiner, Stress Corrosion Cracking in Martensitic High Strength Steels, Technical Documentary Report No. AFML-TR-64-325, Air Force Materials Laboratory, February 1965.

2. Mackay, T. L. and C. B. Gilpin, Stress Corrosion Cracking of Titanium Alloys at Ambient Temperature in Aqueous Solutions, Report SM-49105-Q2, NAS 7-488, January 1967.

3. Hatch, A. J., H. W. Rosenberg, and E. F. Erbin, "Effects of Environment on Cracking in Titanium Alloys," presented at ASTM Pacific Area National Meeting, Seattle, November 1965.

4. Strawley, J. E. and W. F. Brown, Jr., "Fracture Toughness Testing," NASA TN D-2599, January 1965.

5. Brown, B. F. and C. D. Beachem, Corrosion Science, 5, 745 (1965).

6. Phillips, A., V. Kerlins, and B. V. Whiteson, Electron Fractography Handbook, ML-TDR-64-416, AFML-Wright Patterson AFB, January 1965.

7. Avery, C. H. and R. V. Turley, Chloride Stress Corrision Susceptibility of High Strength Steel, Titanium Alloy and Superalloy Sheet, Technical Documentary Report No. AFML-TR-64-44, Vol. I, March 1964 and Vol. II, May 1964.

8. Beck, T. R., Stress Corrosion Cracking of Titanium Alloys, Contract NAS 7-489, Quarterly Progress Report No. 2, December 1966.

9. Howe, D. G. and R. J. Goode, The Effects of Vacuum Heat Treatment on the Stress Corrosion-Cracking Resistance of Alloys of Titanium, a paper presented at the AIME Annual Meeting, Los Angeles, February 1967.